NASA MEMO 3-17-59W

NASA MEMO 3-17-59W

IN-34
394552

# NASA

# MEMORANDUM

SPACE-TIME CORRELATIONS AND SPECTRA OF WALL PRESSURE

IN A TURBULENT BOUNDARY LAYER

By W. W. Willmarth

California Institute of Technology

NATIONAL AERONAUTICS AND SPACE ADMINISTRATION

WASHINGTON

March 1959

NATIONAL AERONAUTICS AND SPACE ADMINISTRATION

MEMORANDUM 3-17-59W

# SPACE-TIME CORRELATIONS AND SPECTRA OF WALL PRESSURE IN A TURBULENT BOUNDARY LAYER

By W. W. Willmarth

## SUMMARY

Measurements of the statistical properties of the fluctuating wall pressure produced by a subsonic turbulent boundary layer are described. The measurements provide additional information about the structure of the turbulent boundary layer; they are applicable to the problems of boundary-layer induced noise inside an airplane fuselage and to the generation of waves on water.

The spectrum of the wall pressure is presented in dimensionless form. The ratio of the root-mean-square wall pressure to the free-stream dynamic pressure is found to be a constant $\sqrt{\overline{p^2}}/q_\infty = 0.006$ independent of Mach number and Reynolds number. In addition, space-time correlation measurements in the stream direction show that pressure fluctuations whose scale is greater than or equal to 0.3 times the boundary-layer thickness are convected with the convection speed $U_c = 0.82U_\infty$ where $U_\infty$ is the free-stream velocity and have lost their identity in a distance approximately equal to 10 boundary-layer thicknesses.

## INTRODUCTION

The experiments to be described were motivated by an interest in the problem of aerodynamic noise generated by the fluctuating fluid flow in a turbulent boundary layer. However, the results of these experiments are applicable to other problems. For instance, they add to our knowledge of the structure of the turbulent boundary layer. They are also applicable to the problem of the generation of waves on water by a turbulent wind as discussed by Phillips in his excellent paper, reference 1.

There are two mechanisms for the generation of noise by a turbulent boundary layer. The first mechanism is singled out when the wall is considered to be perfectly rigid. Then, aerodynamic noise can be generated in the flow field only by the rapid changes of the fluid properties within the turbulent boundary layer. This first problem of boundary-layer noise generation without motion of the wall has been discussed by Phillips in references 2 and 3 and by Curle in reference 4. Experiments by the author (ref. 5) have shown that no appreciable noise is generated directly by the turbulent boundary layer when the wall is rigid and the free-stream Mach number is less than 1/2. However, Dr. John Laufer has recently found and reported in an unpublished communication indications that at supersonic speeds $M \approx 3$ appreciable acoustic radiation is produced by the turbulent boundary layer on the rigid walls of the test section of the 20-inch tunnel of the Jet Propulsion Laboratory.

The present experiments have been designed to apply primarily to the second mechanism of sound generation which occurs when the wall is not rigid. Then, in addition to the sound field produced directly by the fluctuating fluid flow, the fluctuating static pressure in the boundary layer causes deflection of the wall normal to itself. The wall acts like the diaphragm of a loud speaker and radiates sound into the flow field and into the air on the opposite side. It should be emphasized that the amplitude of the wall motion must be small compared with the boundary-layer thickness in order that the boundary layer will not be appreciably affected by motion of the wall. A theoretical treatment of this second mechanism of sound generation has been given by Corcos and Liepmann (ref. 6), Ribner (ref. 7), and Kraichnan (ref. 8) in their work concerning noise generated inside an airplane fuselage. Their analyses of the internal noise field are, however, incomplete since the properties of the turbulent flow in the boundary layer are not well enough known to determine the motion of the wall. It is this fact which motivated the present investigation.

In order to assess the magnitude of the noise field inside an airplane fuselage one needs to know the statistical properties of the fluctuating static pressure along the wall. In particular, the correlation in time and in the two spatial directions parallel to the surface of the wall static pressure is needed. Alternatively, one can ask for the Fourier transform of the pressure correlation with respect to the aforementioned temporal and spatial variables.

It was pointed out in references 6 and 7 that the dominant effect in the generation of sound by wall-pressure fluctuations may well be a kind of resonance phenomenon involving the moving waves or ripples in the flexible wall which are produced and amplified by a convected pattern of static-pressure fluctuations in the boundary layer. Indeed, Ribner's analysis supposes that to a first approximation moving ripples in the airplane skin produce a standing wave motion of the skin which is responsible for the entire sound field inside the fuselage.

The same type of resonance phenomenon dominates the theory put forward by Phillips (ref. 1) for the generation of waves on water.

Phillips shows how convected normal pressure patterns in the turbulent wind moving over an initially plane water surface can excite and add energy to certain wavelets whose wave length, direction of motion, and speed of propagation are related to the scale, direction of motion, and convection speed of the normal pressure fluctuations on the water surface.

With these examples in mind, the experimental program was aimed at measurement of the fluctuating wall static pressure within the turbulent boundary layer. The statistical quantities measured were the root-mean-square pressure and spectrum of the pressure at one point and the space-time correlation of the pressure in the stream direction. The measurements were made at various Reynolds numbers and subsonic Mach numbers.

This investigation was carried out at the California Institute of Technology under the sponsorship and with the financial assistance of the National Advisory Committee for Aeronautics. The author wishes to acknowledge the encouragement and advice of Professors H. W. Liepmann and H. S. Ribner. In addition, the use of Dr. G. T. Skinner's time correlator is appreciated and Mr. R. H. Swartley's help in the building and operation of the electronic equipment is gratefully acknowledged.

SYMBOLS

| | |
|---|---|
| $d$ | diameter of sensitive area of pressure transducer, ft |
| $f$ | frequency, cps |
| $M$ | Mach number |
| $p$ | static pressure of fluid, lb/sq ft |
| $\widetilde{p}(\omega)$ | power spectrum of static pressure, sec $(\text{lb/sq ft})^2$ |
| $\overline{p^2}$ | mean-square static pressure, $\int_0^\infty \widetilde{p}(\omega)d\omega$, $(\text{lb/sq ft})^2$ |
| $q$ | dynamic pressure of fluid |
| Re | Reynolds number based on distance downstream of pipe entrance |
| $t$ | time, sec |
| $U$ | velocity of fluid, ft/sec |

| | |
|---|---|
| $U_c$ | convection speed, ft/sec |
| $U_\tau$ | boundary-layer friction velocity, ft/sec |
| $x$ | distance downstream of pipe entrance, ft |
| $y$ | distance normal to pipe wall, ft |
| $\delta$ | boundary-layer thickness, ft |
| $\delta^*$ | boundary-layer displacement thickness, ft |
| $\nu$ | fluid viscosity |
| $\rho$ | fluid density, slugs/cu ft |
| $\tau$ | delay time, sec |
| $\omega$ | angular frequency, $2\pi f$ |
| $(\ )'$ | value when pressure correlation = 0.1 |
| $\overline{(\ )}$ | mean or average value |

Subscripts:

| | |
|---|---|
| opt | optimum |
| 1 | properties at station x |
| 2 | properties at station $x + \Delta x$ |
| $(\ )_\infty$ | free-stream conditions |

## DESCRIPTION OF EQUIPMENT AND METHODS OF MEASUREMENT

### Wind Tunnel

The measurements were made in a specially designed low-noise- and low-turbulence-level wind tunnel which is described in reference 5. The noise level in the tunnel is controlled by the sound insulation lining the walls of a 35-foot air-inlet duct and by a sonic throat downstream of the test region. The sonic throat prevents sound propagation upstream from the diffuser and is also used for speed control.

The test section of the tunnel (fig. 1) consists of a 4-inch-inside-diameter brass pipe. The turbulent boundary layer produced on the inside walls of the first 5 feet of the pipe was used for the present tests. The boundary layer is approximately 3/4 inch thick 5 feet downstream of the pipe entrance. The ratio of boundary-layer thickness to pipe radius is therefore always less than 3/8 so that the experiments also apply to boundary layers developed on flat surfaces.

For the measurements herein reported the boundary layer was tripped at the station $x = 0$ by the admission of air through fine holes of 1/2-millimeter diameter drilled in the pipe wall.

## Pressure Transducer

The measurements of the fluctuating wall pressure were made with barium titanate pressure transducers which were calibrated in a shock tube. A description of their construction and calibration is given in reference 9. The results of the shock-tube calibration showed that the frequency response was uniform from 5 to 50,000 cps, and the sensitivity of the transducers was $0.76 \times 10^{-6}$ v/dyne/sq cm for a transducer using a 0.163-inch-diameter barium titanate disk. A comparison calibration with the 0.163-inch-diameter transducers showed that the sensitivity was $0.185 \times 10^{-6}$ v/dyne/sq cm for a transducer using 0.100-inch-diameter barium titanate disks.

The electrical signal from the transducers was sensed and amplified by a battery-powered cathode-follower input preamplifier and amplified further by another amplifier.

## Statistical Measuring Equipment

The statistical properties of the amplified electrical signals from the pressure transducers were measured with various electronic devices described below.

Root-mean-square measurements.- The root-mean-square measurements of the pressure fluctuations were made with a vacuum-tube voltmeter. This voltmeter is not a true root-mean-square measuring device since it measures the mean modulus of the input signal. It is, however, calibrated to read the true root-mean-square value of a sine-wave input. For inputs of different wave form, the meter reading is in error. The magnitude of the error for the present measurements was ascertained by measuring the root-mean-square values of a few typical pressure-fluctuation signals with a true root-mean-square meter and with the vacuum-tube voltmeter. It was found that the latter readings were always approximately 7 percent below the true root-mean-square values of the signals. The readings reported herein were measured with the vacuum-tube voltmeter and were corrected for the above 7-percent error.

Spectral measurements.- The spectrum of the pressure fluctuations were measured with a constant-band-width wave analyzer. The constancy of the band width of the analyzer was checked at a low and high frequency (see fig. 2) using a sine-wave generator. An electronic counter was used to give the frequency of the sine-wave-generator signal.

For the present measurements the wave-analyzer output was recorded with an oscillograph, and a clockwork mechanism was used to change the center frequency of the pass band. The pass-band center frequency was also recorded on the oscillograph during the spectral measurements.

Space-time-correlation measurements.- An electronic device designed and built by Skinner as described in reference 10 was used to measure the time correlation $\overline{p(x, t - \tau)p(x + \Delta x, t)}$ of two pressure signals. A sample of the pressure signal $p(x, t - \tau)$ from station $x$ is taken at time $t - \tau$ by the correlator and stored in digital form for a certain variable delay time $\tau$. At the time $t$ a sample of the pressure signal $p(x + \Delta x, t)$ from station $x$ is obtained and multiplied by the previous stored sample. The products $p(x, t - \tau)p(x + \Delta x, t)$ of many repetitions of the sampling process are then averaged to give the correlation between the pressure signals. The products of the sampled signals are formed quite simply by turning on the second signal $p(x + \Delta x, t)$ for a short time which is proportioned to the first, stored signal $p(x, t - \tau)$. The sample products then appear as tiny bursts of power and are averaged by measuring the rate of increase of electrical charge on a capacitor with very low leakage.

The average time required to obtain the two samples of the pressure signals is approximately 50 microseconds which is therefore the minimum delay time that one can obtain with the correlator. The finite sampling time (approximately 25 microseconds for one sample) sets a resolution limit on the frequency of the signals for which one can measure the time correlation. For instance, if one attempts to measure the autocorrelation of a sine wave accurately, the sampling time must be less than one half period. Thus, one should not expect to be able to form an accurate autocorrelation measurement with the correlator on sine waves of more than $f = \frac{1}{(2)(25 \times 10^{-6})} = 20$ kilocycles per second.

The correlator was calibrated and its operation checked by forming the autocorrelation of sine waves. Examples of the correlator performance are shown in figure 3 for sine waves of frequencies of 2.9 and 15 kilocycles per second. It can be seen that the correct value of the autocorrelation, $\cos 2\pi f\tau$, was obtained.

## DISCUSSION OF EXPERIMENTS AND RESULTS

The validity of the pressure measurements to be discussed rests on the conclusion (ref. 5) that the sound radiated by the subsonic turbulent boundary layer is of small intensity. In reference 5 measurements of the wall-pressure fluctuations in a laminar and turbulent boundary layer showed that at subsonic speeds below $M \approx 0.5$ the pressure fluctuations produced by radiated sound from a turbulent boundary layer are completely negligible compared with the local pressure fluctuations within the turbulent layer. Thus, the wall-pressure measurements reported here are caused only by the local pressure field within the boundary layer.

### Boundary-Layer Velocity Profiles

The boundary layer was tripped by admission of air through small holes at the station $x = 0$. The velocity profile was then measured at Mach numbers 0.33 and 0.65 at five axial stations along the pipe surface. Typical boundary-layer profiles for a low and a high Mach number and Reynolds number are presented in figure 4 for comparison with the law of the wall and the law of the wake, using the empirical constants proposed by Coles in reference 11 for a two-dimensional boundary layer with zero pressure gradient. The agreement with Coles' general formulation of the boundary-layer properties means that the boundary layers on the pipe wall are typical of the turbulent boundary layer that would be developed on a flat plate with zero pressure gradient. The displacement thickness was calculated for each profile and used to reduce certain of the results of the pressure measurements to dimensionless form.

### Root-Mean-Square Wall-Pressure Measurements

The root-mean-square wall-pressure measurements were made with a 0.10-inch-diameter transducer that was calibrated by comparison with the 0.163-inch-diameter transducers which had been calibrated in the shock tube as described in reference 9. These measurements were also made at two subsonic Mach numbers (approximately 0.33 and 0.65) and at five axial stations along the pipe wall.

The results are shown in dimensionless form in figure 5. The size of the transducer is appreciable in comparison with the boundary-layer thickness for some of these measurements. For instance, when $d/\delta^* = 4$, $d \approx \delta/2$ where $\delta \approx 8\delta^*$, an appreciable loss in transducer response to the pressure fluctuations is caused by cancellation of the smaller scale fluctuations over the finite area of the transducer face. However, as $d/\delta^*$ decreases the response increases to a value $\sqrt{\overline{p^2}}/q_\infty = 5.5 \times 10^{-3}$ at $d/\delta^* = 1 (d \approx \delta/8)$ and should rise to $\sqrt{\overline{p^2}}/q_\infty = 6 \times 10^{-3}$ as $d/\delta \rightarrow 0$. Thus, one should expect that the magnitude of the root-mean-square wall-pressure fluctuations is $6 \times 10^{-3} q_\infty$. This result is higher than the previous measured result, $\sqrt{\overline{p^2}}/q_\infty = 3.5 \times 10^{-3}$ (ref. 5), in which a larger transducer (0.187-inch diameter) with a resonance at 6 kilocycles was used. The resonance peak at 6 kilocycles with the old transducer was apparently so large that the variation of $\sqrt{\overline{p^2}}/q_\infty$ with $d/\delta^*$ could not be detected. This conclusion is also indicated by the fact that no systematic changes in the spectra of the wall pressure were detectable when the old transducer was used (ref. 5).

## Spectral Measurements of Wall Pressure

The spectral measurements of the wall pressure were made with the same 0.10-inch-diameter transducer as was used for the root-mean-square measurements. An absolute calibration of the wave analyser was made using a random noise generator producing "white" noise and a variable-band-pass filter. Since the spectral density of white noise is constant, the absolute calibration of the wave-analyzer reading was obtained by measuring the mean-square output of the filtered white noise and dividing by the width of the pass band of the Krohn-Hite filter, which is about 30 kilocycles.

The spectra of the pressure were measured at the same Mach numbers and stations along the pipe axis as were the root-mean-square pressure measurements. The spectra are plotted in figure 6 in dimensionless form. The dimensionless spectral parameters used are those proposed in reference 5, and it is necessary to assume that the ratio of the mean-square pressure to the dynamic pressure squared is a constant:

$$\frac{\overline{p^2}}{{q_\infty}^2} = \text{Constant} = \int_0^\infty \frac{\tilde{p}(\omega)d\omega}{{q_\infty}^2} \qquad (1)$$

If the dimensionless frequency is introduced

$$\frac{\overline{p^2}}{q_\infty^2} = \text{Constant} = \int_0^\infty \frac{U_\infty \tilde{p}\left(\frac{\omega\delta^*}{U_\infty}\right)}{\delta^* q_\infty^2} d\left(\frac{\omega\delta^*}{U_\infty}\right) \tag{2}$$

one concludes that the nondimensional spectral density

$$\frac{U_\infty \tilde{p}(\omega)}{\delta^* q_\infty^2} = f\left(\frac{\omega\delta^*}{U_\infty}\right) \tag{3}$$

depends only on the dimensionless frequency $\omega\delta^*/U_\infty$.

The nondimensional spectral density is plotted as a function of $\omega\delta^*/U_\infty$ in figure 6. For $\omega\delta^*/U_\infty \leq 0.3$ the value of $U_\infty \tilde{p}(\omega)/\delta^* q_\infty^2$ is approximately $3.5 \times 10^{-5}$, however, at larger values of $\omega\delta^*/U_\infty$ the values of $U_\infty \tilde{p}(\omega)/\delta^* q_\infty^2$ depend upon the value of $d/\delta^*$. This behavior is caused by cancellation of the small-scale (high-frequency) pressure fluctuations on the face of the transducer. For larger values of $d/\delta^*$ the spectral density is reduced at high frequencies; however, for smaller values of $d/\delta^*$ the spectral density is not as low at high frequencies. From figure 6 it appears that the nondimensional spectra would approach a universal curve if $d/\delta^* \longrightarrow 0$. Note that the above behavior is consistent with the results of the root-mean-square pressure measurements. (See section entitled "Root-Mean-Square Wall-Pressure Measurements.")

The data of figure 6 appear to have considerable scatter. However, the spectra were measured by sweeping the pass-band center frequency slowly from low to high frequencies at a speed of 200 cps/sec. The wave-analyzer output was smoothed with a capacitor; however, output fluctuations were still present. Thus, the points shown in figure 6 can exhibit scatter due to insufficient averaging time. In addition, all errors including averaging errors in the spectral measurements are shown doubled in figure 6 since the wave-analyzer output was squared after the spectra were measured.

## Space-Time Correlation Measurements

The space-time correlation was measured at three free-stream Mach numbers, 0.333, 0.456, and 0.672, at a station 3.8 feet downstream of the pipe entrance. The two pressure transducers used were those described in reference 9 with a diameter of 0.163 inch, which were somewhat larger than the 0.10-inch-diameter transducer used for the spectra and root-mean-square measurements. For these correlation measurements, the ratio $d/\delta \approx 0.3$ and the results will apply only to pressure fluctuations whose size is $\gtrsim 0.3\delta$. Smaller scale pressure fluctuations will partially cancel each other on the transducer face. The two transducers were mounted in the pipe wall with one directly downstream of the other. The transducer spacing $\Delta x$ was 0.125, 0.25, and 0.50 foot for each set of measurements at a given Mach number.

The results of the measurements of the space-time correlation of the pressure are shown in figures 7(a), 7(b), and 7(c), for which the correlation has been normalized by the factor $\sqrt{\overline{p_1^2}}\sqrt{\overline{p_2^2}}$. For each spacing and free-stream Mach number there is an optimum time delay $\tau_{opt}$ at which the correlation is a maximum. The ratio $\Delta x/\tau_{opt}$ was found to be approximately $0.82U_\infty$ for the nine measurements. The ratio $\Delta x/\tau_{opt} = 0.82U_\infty$ is the average speed at which wall-pressure disturbances in the turbulent boundary layer are convected. The value $\Delta x/\tau_{opt} = 0.88U_\infty$ at Mach number 0.672 of figure 7(a) is slightly higher than the average speed; however, further measurements at higher Mach numbers would be required to show that this increase in the convection speed is significant.

In addition, the data in figures 7(a) 7(b), and 7(c) show that the space-time correlation has decreased by a factor of 10 in a time $\tau'$ given by the relation

$$\frac{\tau' U_\infty}{\delta^*} \approx 100$$

From the average convection speed of the disturbances $U_c = 0.82U_\infty$, the distance $\Delta x'$ in which the maximum of the space-time pressure correlation decreases by a factor of 10 is

$$\Delta x' = \tau' U_c \approx 80\delta^*$$

and since $\delta \approx 8\delta^*$ this distance is

$$\Delta x' \approx 10\delta$$

Thus, the convected pressure fluctuations have lost their identity after being carried downstream a distance equal to approximately 10 times the boundary-layer thickness.

The pressure correlation shown in figure 7 has decreased to approximately one-half when the streamwise distance separating the pressure transducers is $\Delta x/\delta \approx 2.0$. Measurements of space-time correlations of the streamwise velocity component in a turbulent boundary layer by Favre, Gaviglio, and Dumas (ref. 12) indicate that the velocity correlation has dropped to a value of one-half when $\Delta x/\delta = 2.4$. One cannot compare the velocity and pressure correlations directly since the wall pressure is produced by velocity fluctuations throughout the boundary layer. However, it is gratifying to note the order of magnitude of the agreement between the velocity- and pressure-correlation measurements. As a matter of fact, for $y/\delta = 0.24$ the ratio $U/U_\infty = 0.78$ which again agrees with the convection velocity for the pressure fluctuations, $U_c/U_\infty = 0.82$. For points nearer the wall such as $y/\delta = 0.06$, Favre, Gaviglio, and Dumas find that the maximum velocity correlation is one-half for $\Delta x/\delta = 1.2$. Since $\Delta x/\delta$ is less than 2 at $y/\delta = 0.06$ and since $U/U_\infty \approx 0.63$ at this point, it seems reasonable to propose that the bulk of the convected pressure fluctuations measured here are caused by the larger scale eddies in the boundary layer. On the other hand, this is to be expected since $d/\delta \approx 0.3$ and the minimum size of the pressure fluctuations that can be measured is of the order of $0.3\delta$.

Additional measurements using smaller transducers are desirable. One could filter out the low-frequency, large-scale fluctuations and determine the convection speed and other properties of the small-scale pressure fluctuations. Also, nothing is yet known about the scale of the presssure fluctuations normal to the stream direction.

## CONCLUSIONS

The following conclusions were drawn from an investigation of the space-time correlations and spectra of wall pressures in a turbulent boundary layer:

1. The root-mean-square wall-pressure fluctuations approach the value $\sqrt{\overline{p^2}} = 0.006q_\infty$ as $d/\delta \rightarrow 0$ (where $q_\infty$ is the free-stream pressure, $d$ is the diameter of the pressure transducer, and $\delta$ is the boundary-layer thickness) and are independent of Reynolds number and Mach number at subsonic speeds.

2. The spectra of the wall pressure can be thrown into a dimensionless form. The dimensionless spectra apparently approach a universal function of $\omega\delta^*/U_\infty$ (where $\omega$ is the angular frequency, $\delta^*$ is the boundary-layer displacement thickness, and $U_\infty$ is the free-stream velocity) as the transducer size is reduced.

3. Space-time correlation measurements of the pressure fluctuations whose scale is greater than or equal to $0.3\delta$ show that a given pressure pattern is convected with a speed $U_c = 0.82U_\infty$ and is essentially destroyed in a distance of 10 boundary-layer thicknesses (e.g., in a time $\tau' \approx 100\delta^*/U_\infty$).

California Institute of Technology,
Pasadena, Calif., April 10, 1958.

REFERENCES

1. Phillips, O. M.: On the Generation of Waves by Turbulent Wind. Jour. Fluid Mech., vol. 2, pt 5, July 1957, pp. 417-445.

2. Phillips. O. M.: Surface Noise From a Plane Turbulent Boundary Layer. Rep. No. 16, 963/F.M. 2099, Brit. A.R.C., Aug. 4, 1954.

3. Phillips. O. M.: On the Aerodynamic Surface Sound from a Plane Turbulent Boundary Layer. Proc. Roy. Soc. (London), ser. A, vol. 234, no. 1198, Feb. 21, 1956, pp. 327-335.

4. Curle, N.: The Influence of Solid Boundaries Upon Aerodynamic Sound. Proc. Roy. Soc. (London), ser. A, vol. 231, no. 1187, Sept. 20, 1955, pp. 505-513.

5. Willmarth, W. W.: Wall Pressure Fluctuations in a Turbulent Boundary Layer. NACA TN 4139, 1958.

6. Corcos, G. M., and Liepmann, H. W.: On the Transmission Through a Fuselage Wall of Boundary Layer Noise. NACA TM 1420, 1956.

7. Ribner, H. S.: Boundary-Layer-Induced Noise in the Interior of Aircraft. UTIA Rep. No. 37, Inst. of Aerophysics, Univ. of Toronto, Apr. 1956.

8. Kraichnan, R. H.: Noise Transmission from Boundary Layer Pressure Fluctuations. Jour. Acous. Soc. Am., vol. 29, no. 1, Jan. 1957, pp. 65-80.

9. Willmarth, W. W.: Small Barium Titanate Transducer for Aerodynamic or Acoustic Pressure Measurements. Contract NAw-6479, NACA and Calif. Inst. of Tech., May 1957.

10. Skinner, G. T.: Time Correlator for Problems in Aerodynamics. NACA TN 3682, 1956.

11. Coles, Donald: The Law of the Wake in the Turbulent Boundary Layer. Jour. Fluid Mech., vol. 1, pt. 2, July 1956, pp. 191-226.

12. Favre, A. J., Gaviglio, J. J., and Dumas, R. J.: Further Space-Time Correlations of Velocity in a Turbulent Boundary Layer. Jour. Fluid Mech., vol. 3, pt. 4, Jan. 1958, pp. 344-356.

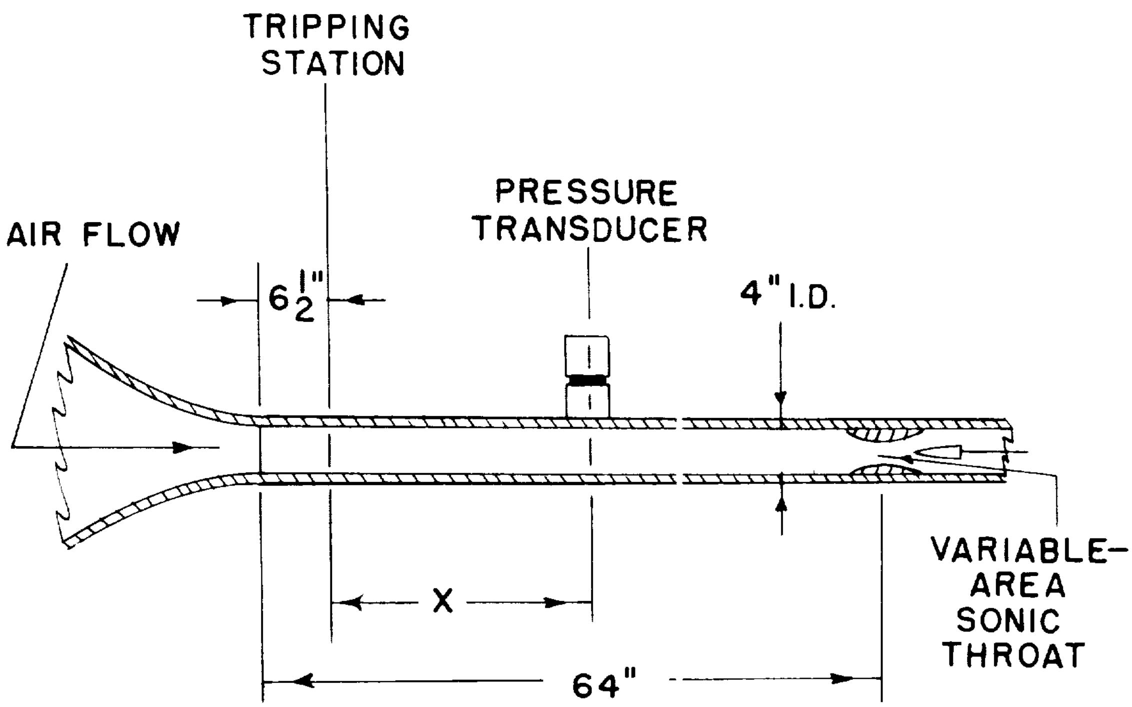


Figure 1.- Pipe test section.

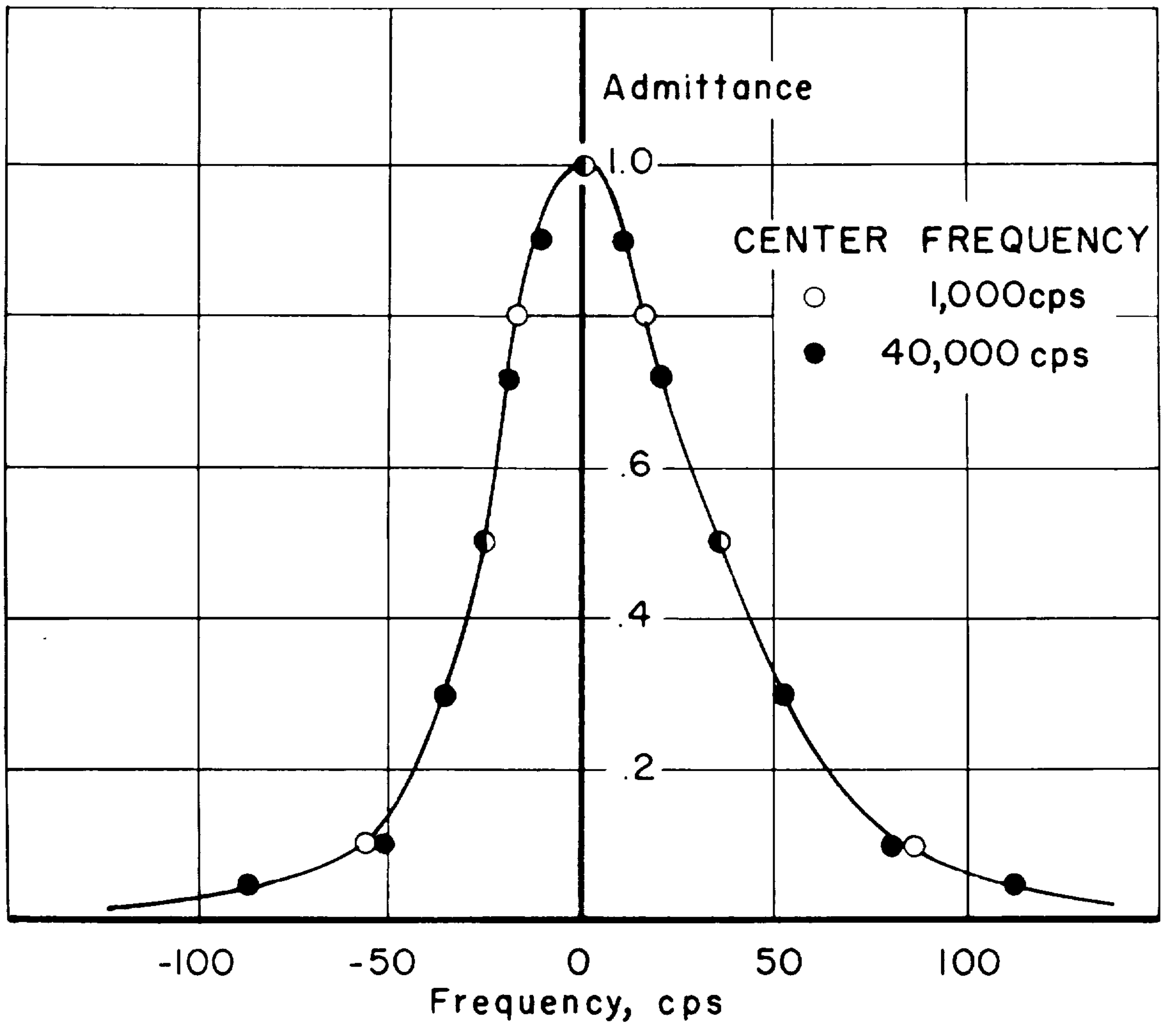


Figure 2.- Band-pass characteristics of wave analyser used in experiments.

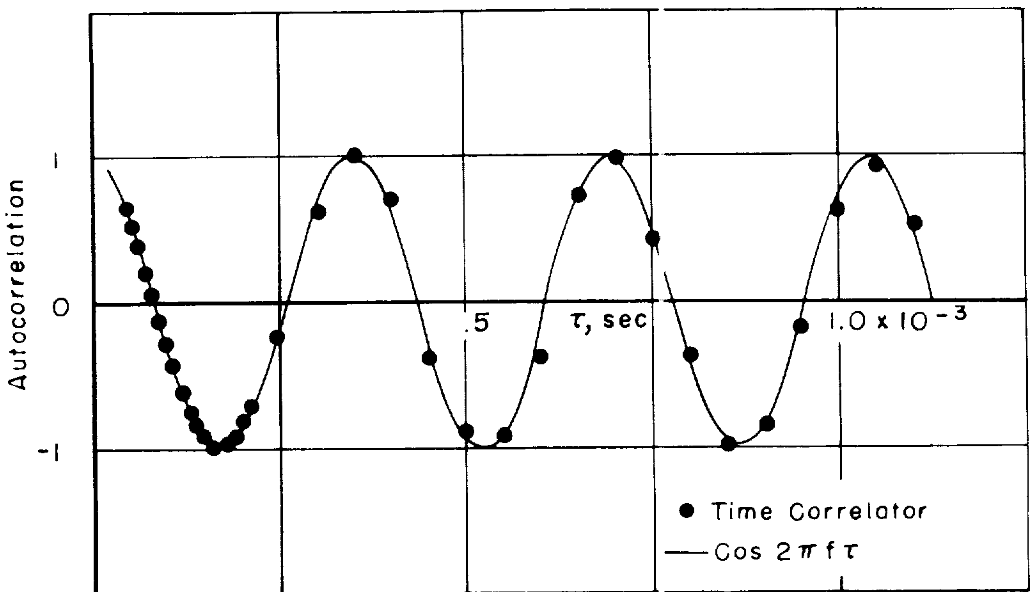


(a) f = 2,900 cps.

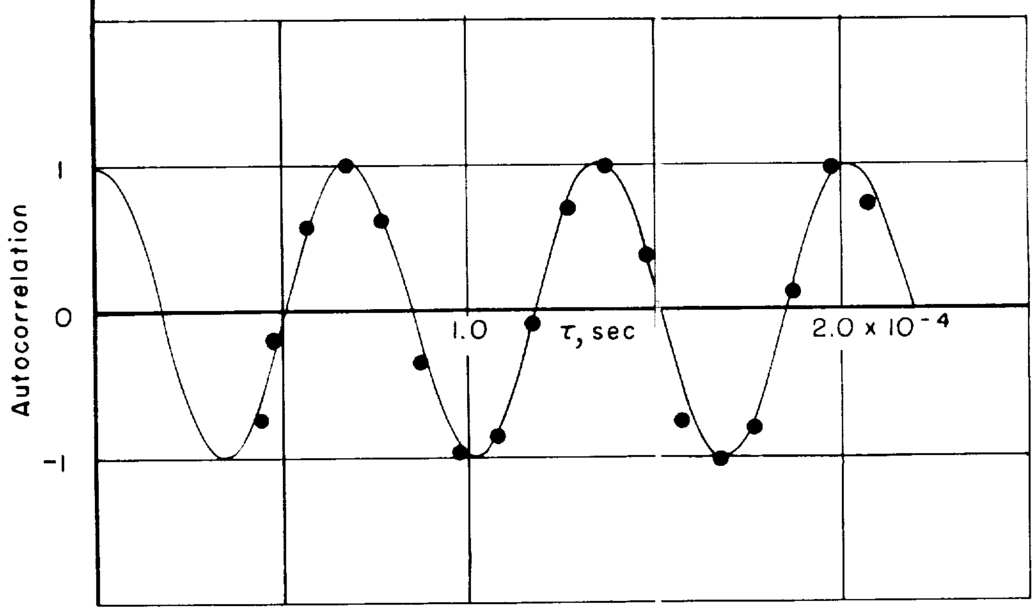


(b) f = 15,000 cps.

Figure 3.- Check of time-correlator performance by autocorrelation of sine waves.

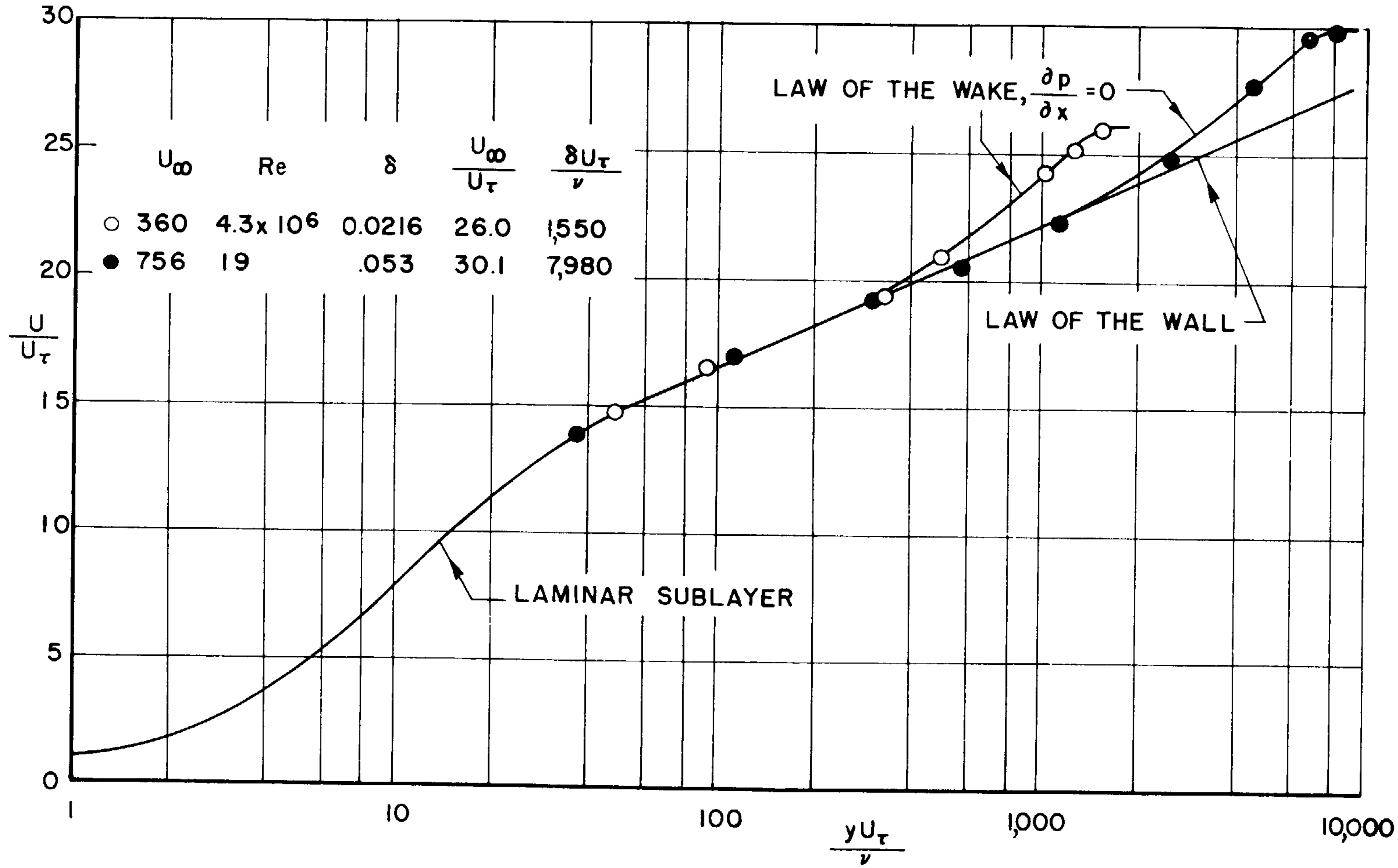


Figure 4.- Typical velocity profiles of turbulent boundary layer developed on wall of pipe.

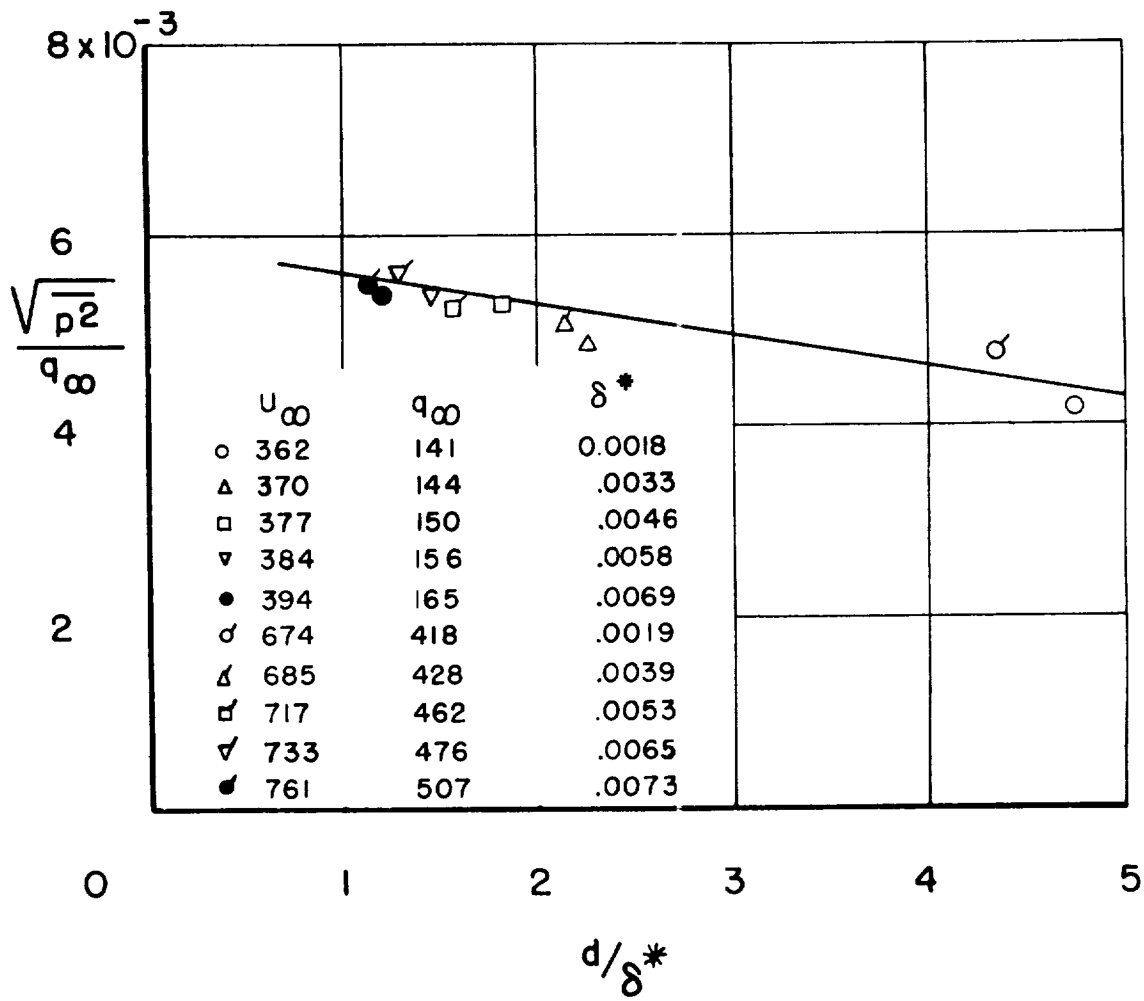


Figure 5.- Root-mean-square wall pressure in a turbulent boundary layer.

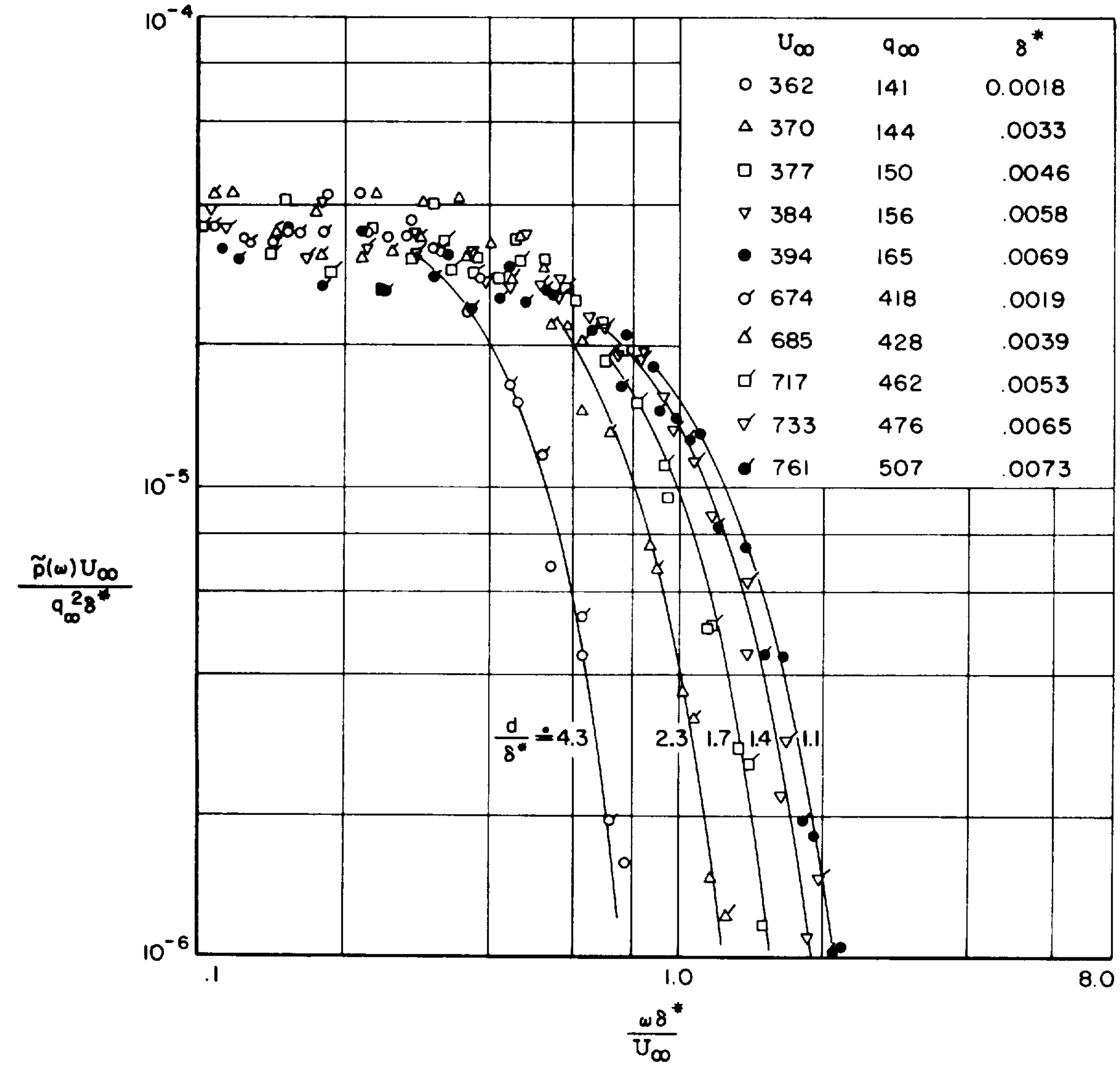


Figure 6.- Power spectra of fluctuating wall pressure in a turbulent boundary layer.

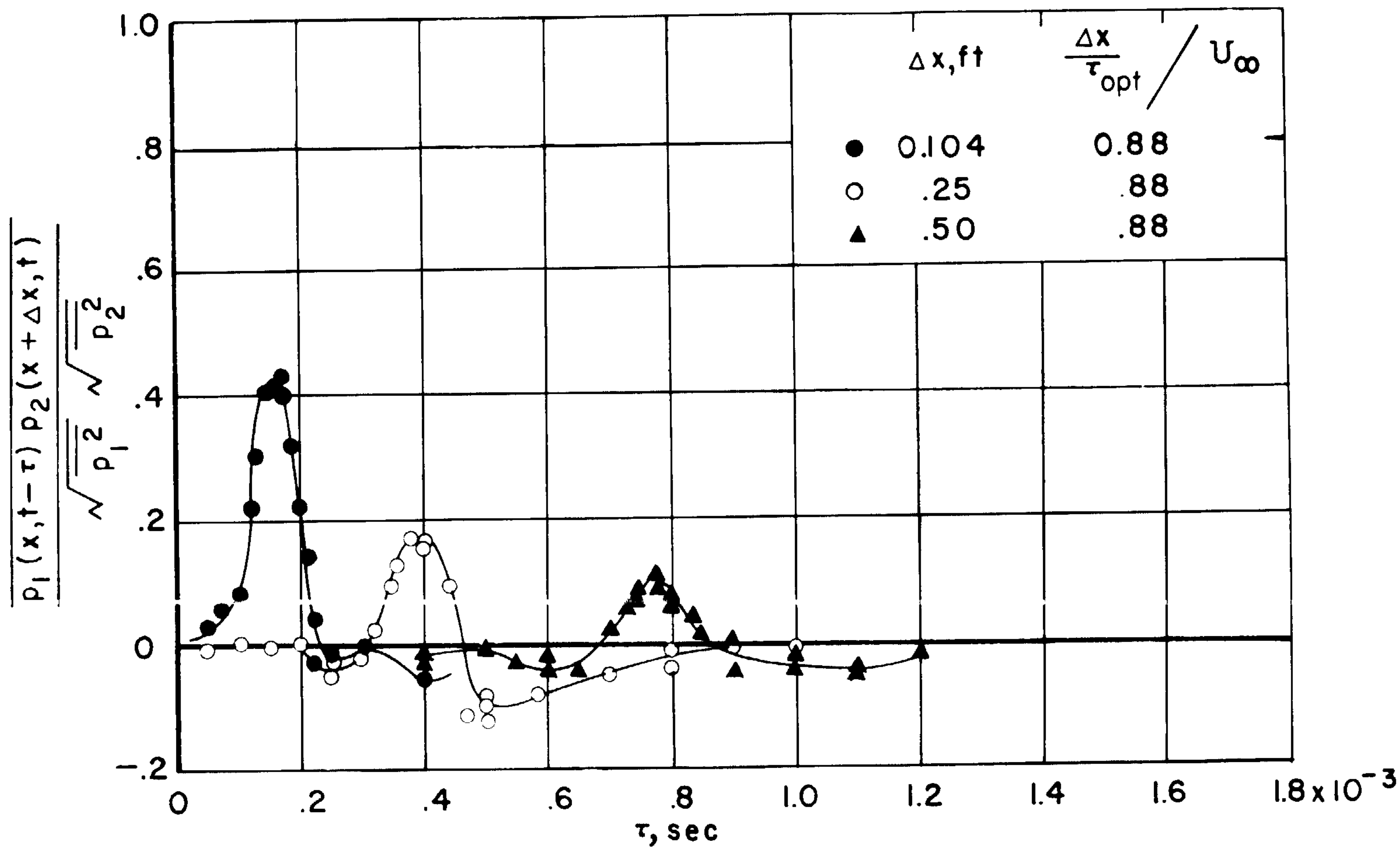


(a) $M_\infty = 0.672$; $U_\infty = 738$ feet per second; $\delta^* = 0.0065$ foot.

Figure 7.- Space-time correlations of pressure.

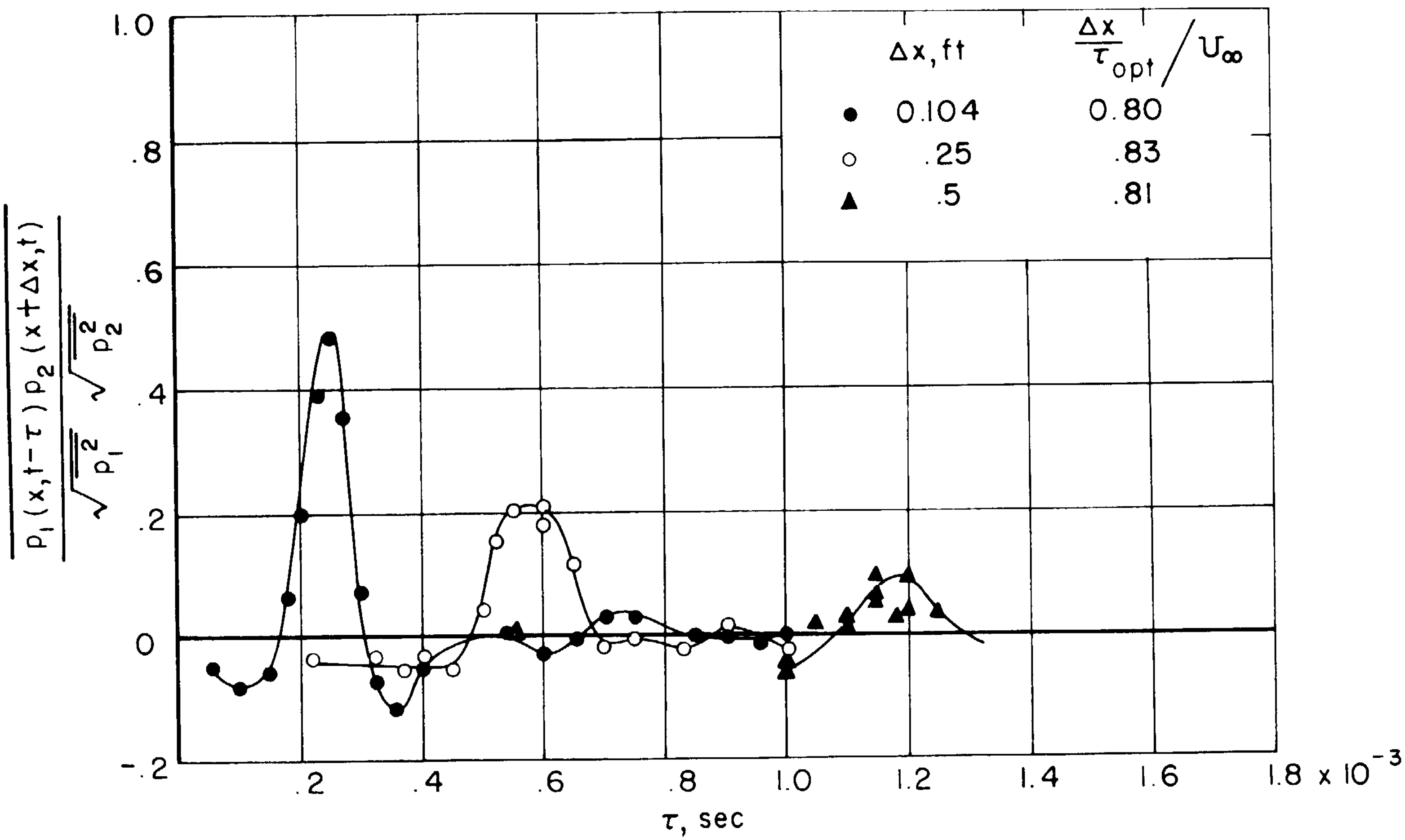


(b) $M_\infty = 0.465$; $U_\infty = 524$ feet per second; $\delta^* = 0.0061$ foot.

Figure 7.- Continued.

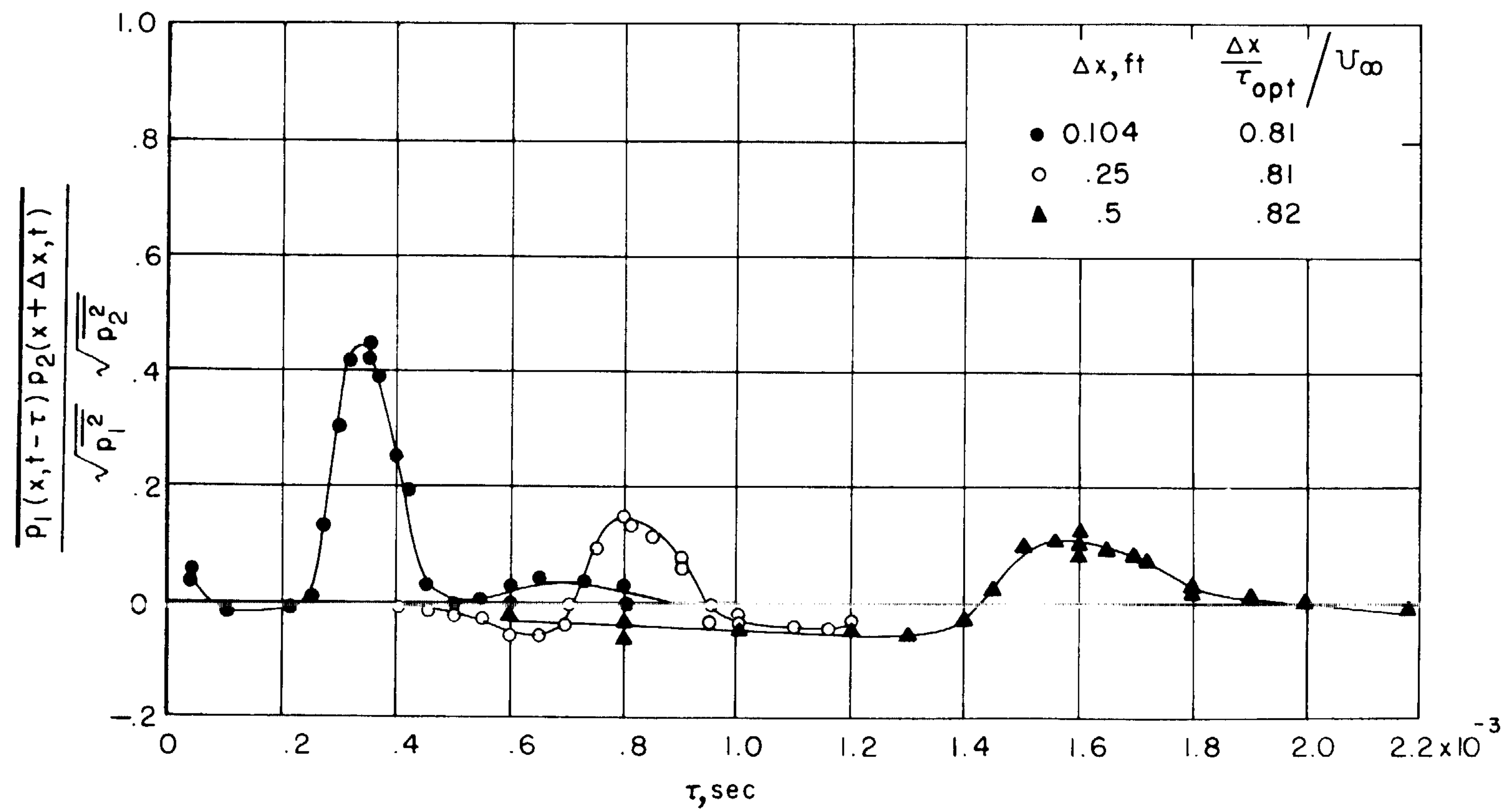


(c) $M_\infty = 0.333$; $U_\infty = 378$ feet per second; $\delta^* = 0.0058$ foot.

Figure 7.- Concluded.